BARRY E. GRABOW, BRADLEY G. BOONE, and RAYMOND M. SOVA

MODELING AND ANALYSIS OF HIGH-TEMPERATURE SUPERCONDUCTING THIN-FILM DETECTORS

A model appropriate for computer simulation of a high-temperature superconducting detector's responses to microwaves and visible light has been developed at the Applied Physics Laboratory. This model will be used to approximate the responses of a bismuth-strontium-calcium-copper oxide detector to microwave frequency and helium-neon laser light over a wide temperature range (from zero up to the critical transition temperature of the superconductor) on the basis of microscopic theoretical results. The nonbolometric (microwave) detection mode is emphasized here because it is faster and more sensitive than the bolometric (helium-neon) mode, which is already well understood.

INTRODUCTION

Superconductivity has recently returned to the forefront of promising microelectronic technologies with the discovery of high-temperature superconductors. When Bednortz and Müller observed "possible high T_c superconductivity in the BaLaCuO system,"[1] they spurred a research explosion in superconductivity that pushed the critical temperature T_c over 130 K, which is well within the range of nitrogen-refrigerated systems. This new threshold in temperature has opened up fields of science and technology to novel superconductor applications. An unprecedented opportunity exists to exploit this technology and apply high-temperature superconducting (HTSC) materials to microelectronic circuits.

One of the most likely outcomes of recent breakthroughs in the field of superconductivity will be the development of HTSC thin-film devices for electro-optical and radio-frequency sensors.[2,3] Among the many possibilities being considered, passive thin-film devices, such as detectors of electromagnetic radiation for use in electro-optical and electronic systems, are favored. Recent investigations by the authors have shown that granular film (multiple Josephson junction) detectors may be competitive with conventional Schottky diode detectors in the microwave spectral region because of the fast response times and high sensitivities associated with multiple weakened superconducting regions between grains of the film.

Our previous work on this topic[4-6] shows that both bolometric and nonbolometric detection modes can be observed in the same bismuth-strontium-calcium-copper oxide samples under mutually exclusive conditions: bolometric with helium-neon (HeNe) laser light (633 nm) and nonbolometric with microwaves (9 GHz). Investigations of the nonbolometric detection mode in those granular thin films show a response peak occurring at a lower temperature and well separated from the bolometric peak. Measurements indicate that the nonbolometric mode is faster and more sensitive than the bolometric mode. Analysis of the microwave response, including variations of temperature, current, power, and sample granularity, supports the model of direct coupling of radiant energy to weak links in these granular films. Empirical data show an increase in response for films with larger sheet resistances and transition widths. Laser modification of thin films yields greater responses, which can be attributed to altered film morphology.

We present recent modeling of these measured results and show that the observation of noise emission peaks in unilluminated films can be explained by a thermal fluctuation voltage occurring in the networks of Josephson junctions inherent in these films. Strong correlation between noise voltage peaks in unilluminated films and microwave response peaks in illuminated films implies that the response is a fluctuation voltage enhancement by microwaves. The breaking of superconducting electron pairs (pair breaking) caused by microwave illumination of weakened superconducting regions between film grains can generate photoexcitation current, which enhances the thermal fluctuation voltage. A computer simulation of the response of an array of weakly coupled superconducting connections between strongly coupled superconducting grains is compared with our measured microwave response. In this response model, the visible light component is based on bolometric effects, and the microwave component is based on Josephson junction detection.

Our present work shows that a junction model predicated on the thermal fluctuation voltage can be used to characterize our measured data. The results of this modeling give valuable information for the application of the nonbolometric detection mode to detectors. The junction model of the microwave response will be useful in predicting the response of a film with a controlled granular structure when the number, size, and characteristics of the grains are known. If the growth of superconducting grains and junctions can be controlled (by laser patterning, annealing, or growth of superconductor/normal metal/superconductor [SNS] junctions, for instance), it may be

possible to optimize the nonbolometric response for detector applications with this response model.

DETECTORS AND MECHANISMS

One may characterize all noncoherent detectors as devices wherein a measurable parameter of that device changes in a predictable way in response to incident electromagnetic radiation, and this information can thus be used to determine the energy in the incident signal.[7] Power detectors can then be classified by the parameter changed by incident radiation.

Superconductors have been studied for use as radiation detectors by many researchers, and many detector designs have been investigated.[8-15] Superconducting detectors of radiant energy use the dependence of resistance on temperature or current as a detection mechanism.[16] This change of resistance is measured as an alteration of sample voltage. A typical HTSC detector configuration is described in Reference 4. The next two sections present a simplified model of the response process appropriate for computer simulation of an HTSC detector's responses to microwaves and visible light.

Voltage Response Equation

The voltage response expression given as Equation 1 is the starting point for a model that incorporates the essential microscopic phenomena in HTSC materials. In general, a voltage change may be induced in a superconductor by two well-known methods: the first is a thermal response mode referred to as the bolometric mode; the second is a current response mode called the nonbolometric mode. Thus, the total change in voltage induced in a small piece of superconductor is expressed in the following two terms, as shown by Bertin and Rose:[8]

$$dV = \frac{\partial V}{\partial T} dT + \frac{\partial V}{\partial I} dI, \qquad (1)$$

where the first term represents the bolometric response, the second term denotes the nonbolometric response, and where

V = detected voltage (V),
T = temperature of detector (K),
$I = I_B + I_L + I_F$ = total current (A),
I_B = bias current (A),
I_F = fluctuation quasiparticle current (A), and
I_L = photoexcitation quasiparticle current (A).

The temperature and current are independent variables and are functions of initial conditions (bias temperature and bias current) and applied incident power. This approach assumes that the fluctuation current is not affected by microwave heating (i.e., that the microwave heating is small enough to have a negligible effect on I_F and that I_F is a function of initial bias current and initial temperature). The photocurrent created by the microwaves is considered to be included only in the I_L term.

Manipulating the bolometric term to show its dependence on thermal conductance, resistance, and bias current, and expanding the nonbolometric term into a form that shows its dependence on the gap parameter and critical current (the total current variable is now contained in the $\partial V/\partial P$ factor),[5] yield

$$\frac{dV}{dP} = I_B \frac{\partial R}{\partial T} \frac{1}{G(T)} + \frac{\partial V}{\partial I_c} \frac{\partial I_c}{\partial \Delta} \frac{\partial \Delta}{\partial P}, \qquad (2)$$

where

P = applied incident power (W),
$G(T)$ = thermal conductance of sample and substrate (W/K),
I_B = bias current (A),
I_c = critical current (A),
Δ = superconducting energy gap (W), and
R = resistance of sample (Ω).

The response is now written in a general form consisting of the sum of two terms, each identical to those given by Farrell.[9] In contrast to Farrell's approach, these two terms have been derived simultaneously from a common point, resulting in a single equation showing the voltage response as the weighted sum of the bolometric and nonbolometric effects. In Equation 2, the first term represents the steady-state bolometric effect and is dependent on the bias current, the slope of the resistive transition, and the inverse of the thermal conductance factor. The second term signifies the nonbolometric voltage response and is dependent on the three factors shown.

As with conventional bolometers, superconducting bolometric detection is caused by a change in a sample's resistivity in response to heating by incident radiation. A superconducting material heated to the critical temperature T_c will go through a transition from the superconducting state to the normal state in a very small temperature interval called the transition width ΔT. The very large $\partial R/\partial T$ that occurs within the transition width region is utilized for bolometric detection.[17] Such a device is called a transition edge bolometer. It is operated by holding its bias temperature fixed at the center of the transition region under background radiation. When an incident signal is present, the bolometer is heated to a higher temperature by incident photons. This heat flux changes the thermal equilibrium of the superconductor, causing Cooper pairs to break and return to quasiparticle states. This process restores the thermal equilibrium, but at a higher temperature, with more normal-state electrons and a corresponding increase in resistance.[18] The resistance change is converted to a voltage change by biasing the device with a constant current source. The bolometric voltage response is directly proportional to $\partial R/\partial T$, as shown in Equation 2.

Although the bolometric effect is well understood and easily modeled, each of the three partial derivative factors of the nonbolometric effect must be investigated to specify a nonbolometric response model. The first two factors of the nonbolometric term ($\partial V/\partial I_c$) and ($\partial I_c/\partial \Delta$) can be evaluated on the basis of the type of junction (discussed in the next section) being modeled in the film, whereas the third factor ($\partial \Delta/\partial P$) depends on the mechanism behind the direct change in the superconducting energy gap due to incident radiant energy. These factors are the subject of analytical investigations and are described in a later section.

Mechanisms of the Nonbolometric Response Model

The appendix, "A Quick Tutorial on Superconductivity," provides the theoretical background for the detection mechanisms. As described earlier, the current mode (the dependence of voltage on current) is responsible for the nonbolometric detection of radiant energy in superconductors. This detection can occur as the result of several mechanisms: directly via the Josephson effect, the breaking of Cooper pairs (electrons of opposite momentum and spin near the Fermi energy condensed into bound pairs) under nonequilibrium conditions,[19,20] classical rectification (video or square-law detection),[15] and fluxon interactions.[20,21] Many recent investigations ascribe the measured results with the HTSC films to a random network of Josephson junctions in which each junction is modeled as having two currents: a supercurrent (Cooper pairs) and a normal current (quasiparticles).[22-28] It is also possible that incident radiation couples to existing vortices created by the bias current and induces increased dissipation.[12,29-33]

Superconducting tunnel junctions are two separate conducting elements, at least one of which must be a superconductor, separated by a thin layer of nonsuperconducting material, most commonly an insulating region, through which both superconducting Cooper pairs and/or nonsuperconducting quasiparticles (normal electrons) may tunnel[34] (Fig. 1). The two most common of these structures are the superconductor/insulator/normal metal (SIN) device and the superconductor/insulator/superconductor (SIS) device. Arrays of junctions can occur naturally in granular thin-film superconductors. Radiant energy can be detected in these junctions, which usually operate in modes using a majority of either quasiparticle current (quasiparticle tunnel junctions) or Cooper pair current (Josephson junctions). The utility of these junctions as detectors is described in the following paragraphs.

One method of detecting radiation in Josephson junctions is pair breaking. In this mechanism, photons with energy above the gap couple directly to the Cooper pairs, providing enough energy to break the pairs and create quasiparticles. These optically broken quasiparticles are described as excess quasiparticles, since they are nonequilibrium particles and would not be in the normal state under thermal equilibrium conditions.[11,19,20] If the junction is biased near the junction critical current, the decrease in the number of Cooper pairs and increase in quasiparticles will decrease the intrinsic critical current and cause a finite voltage to appear across the sample. In the area of the weak-link junction, the energy gap may be suppressed several orders of magnitude owing to weak coupling of the grains. Also, the granularity of the sample could result in a high surface resistance with consequent high absorption of microwave energy. In this way, microwave radiation could give a large response, whereas a bolometric response could be masked.[9]

Farrell[9] models this type of response for a low-capacitance weak-link junction consistent with the resistively shunted junction (RSJ) model to describe its current-voltage and resistive characteristics. Our work models nonbolometric and bolometric responses in the same sample when irradiated with light above the gap. The calculations of the nonbolometric response are based on thermal-flux-averaged voltage equations given by Ambegaokar and Halperin,[10] and quasiparticle density equations derived by Parker[18] and Owen and Scalapino,[35] which are discussed below. We will model the microwave response in our films using this approach.

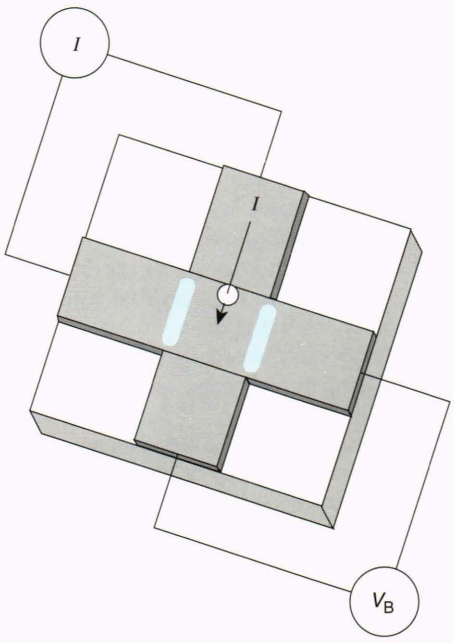

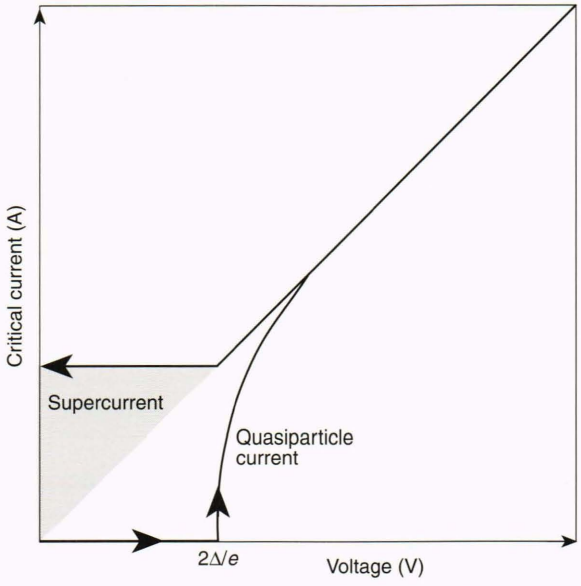

Figure 1. High-capacitance voltage-biased tunnel junction showing hysteresis. (Δ = superconducting energy gap, I = total current, V_B = bias voltage, e = electron charge.)

ASSESSMENT OF GRANULAR THIN-FILM MICROWAVE RESPONSE

Granular thin-film detectors consist of an ensemble of superconducting grains in which the strength of coupling (and associated critical current) varies widely over the

film (see Figs. 2 and 3). When incident radiation couples to such films, the exact mechanism, whether Josephson junction mediated or vortex mediated (or a combination of both), is not always clear.[36-39] To optimize the nonbolometric response of our granular films, a model that fits our observed data (e.g., voltage response versus temperature, current, and field strength) must be found. Some of the parameters that must be considered are the effect of granularity on response; the sample response versus incident power and wavelength, bias current, and temperature; and sample response time.

The response versus temperature for various bias currents and the response versus temperature for various incident powers[4] give evidence for the theory of direct coupling of radiant energy to weak links in granular thin films.[40,41] Results of work by Afanasyev et al.,[26,27] and Strom et al.,[25,33] which model the granular material as a system of grain-boundary weak links with different critical currents, are consistent with our measurements and modeling approach. It is clear that the granularity and associated weak links of a sample have an effect on the response.[23,28,32,42-44] It was not clear, on the basis of previous work, that the increase in response is due solely to Josephson effects. The relative size of the weak links could allow for the effects of vortices to be felt between grains, whereby more fluxons could pass through the weak link, resulting in resistive losses (see Fig. 2). Although several hypotheses have been advanced to explain the microwave response using fluxon-mediated mechanisms, such as Gallop et al.,[30] Voss et al.,[45] Konopka et al.,[22,23] Culbertson et al.,[32] and Jung et al.,[24,46] our model attributes the response to Josephson effects alone, as described in the section on model development.

Observation of microwave response peaks in microwave-illuminated films can be explained by a thermal fluctuation voltage[10] occurring in the networks of Josephson junctions inherent in these films and will be a major component of our model. The strong correlation between the noise peaks in the unilluminated film and the microwave response peaks in the microwave-illuminated film leads us to believe that the nonbolometric response is a thermal fluctuation voltage enhancement by microwaves. In the next section, we will show that the noise peaks observed can be attributed to this thermal fluctuation voltage and that our measured microwave response is consistent with microwave enhancement of the fluctuation voltage noted in our samples.

The assessment of prior work in the field reinforces the ideas that the microwave response is a current mode response, that it depends on the sample granularity and its associated weakened superconducting regions, and that the response can be modeled using a granular film array with inherent Josephson junction properties. It is on these assumptions that our response model is based.

MODEL DEVELOPMENT

Modeling Approach

In our nonbolometric response model, photon–Cooper pair interactions and thermal fluctuations within a weak-link structure having inherent Josephson effect properties will be considered as the microscopic detection mechanism. In the method described by Farrell,[9] an approach utilizing an RSJ model of a weak link with a "thermal-fluctuation-averaged voltage solution"[10] was used to model the nonbolometric effect. This junction model

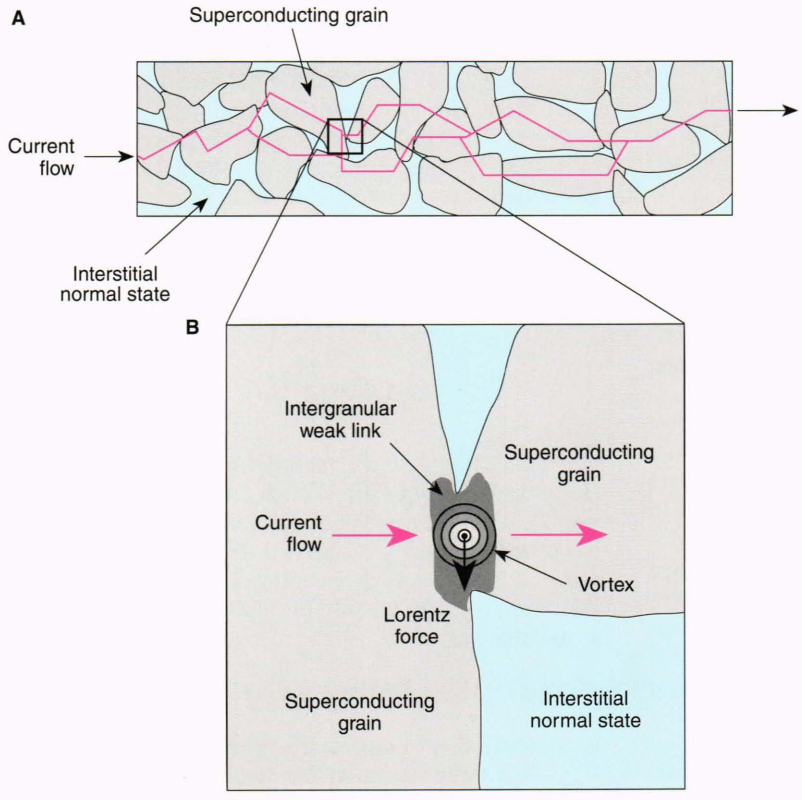

Figure 2. Granular thin-film diagrams. **A.** Bias current percolation path through the film. **B.** Flux motion in the intergranular region due to Lorentz forces.

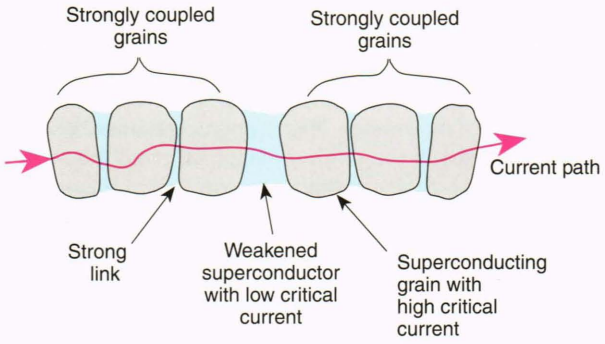

Figure 3. Grain configuration used in nonbolometric model showing strongly coupled grains and a weakened superconducting region.

provides a nonzero thermal noise voltage in the junction that is the basis of the noise response. Microwave illumination may cause a modulation of this noise by breaking Cooper pairs (creating a nonequilibrium state and a corresponding higher effective temperature), resulting in a photocurrent and an enhancement of the thermal fluctuation noise voltage.

We will show that pair breaking in weak links can generate photoexcitation current and cause an increase in the quasiparticle density, resulting in the reduction of the energy gap. The decrease in the energy gap due to excess quasiparticles and photocurrent corresponds to a decrease in the superconducting order parameter, which results in a reduction of the junction critical current and an enhancement of the detected thermal fluctuation noise voltage. In this way, dynamic pair breaking by microwave illumination could be the mechanism driving the fluctuation voltage enhancement of the nonbolometric detection mode. To break a Cooper pair, the photon energy must be on the order of twice the energy gap,[34] given as $\hbar\omega \geq 2\Delta\ (I, T, \mathbf{x})$ for granular films, where $\hbar$ is Planck's constant divided by 2π, ω is the radiation energy in rad/s, and $\mathbf{x}$ is a position vector that describes the energy-gap dependence on location in the film.

Areas of weakened superconductivity exist in granular thin films between grains where the superconducting order parameter will be greatly reduced compared with areas of strong superconductivity. These weakened areas may consist of an ensemble of weak Josephson junctions between the grains. Microwave radiation must interact with these areas of weakened superconductivity to produce quasiparticles by pair breaking, since the photon energy is not on the order of twice the energy gap in a superconductor with strong coupling. If a region is very weakly connected, the order parameter may be reduced far enough to allow microwave pair breaking.

A low-capacitance Josephson junction in a voltage state dominated by thermal fluctuations would show a temperature-dependent thermal fluctuation noise voltage without illumination. When such a junction is illuminated with radiant energy, the Cooper pairs are broken, creating a photoexcitation current (injected quasiparticles) and a resulting lower critical current and increased junction voltage.[4,5] The subsequent temperature dependence of the fluctuation voltage (and current) and photoexcitation current will be described in this section.

The granular film can be pictured as an array of weakly coupled superconducting connections among several superconducting grains joined by strongly coupled weak links, as shown in Figure 3. Both the weakly coupled superconducting connections and the strongly coupled areas between superconducting grains will be represented by the average-voltage solution of the RSJ model, assuming a low-capacitance weak link structure.[10] This approach is valid if one supposes that the grains and the tightly coupled superconducting junctions joining them have high critical currents, whereas the weakened superconductor has a much lower critical current.

Next, since all of the weakly coupled superconducting connections are different, the film will be modeled as a distribution of these granular connections, with the weakened superconductors having various critical currents to produce a spreading effect. This approach can yield a granular film resistance-versus-temperature curve with a wide transition width, a nonvanishing resistive tail, and a microwave response located in the resistive tail region. In addition, and most important, the model can give both bolometric and nonbolometric responses in the same film, as seen in our measurements. The spreading effect will be shown explicitly later.

Fluctuation Voltage Equation

The thermal-fluctuation-averaged voltage solution[47-49] of Ambegaokar and Halperin is

$$\langle V \rangle = 2\frac{I_c R_N}{\gamma\pi}\frac{\sinh(\beta\pi/2)}{\left|I_{j\beta/2}(\gamma/2)\right|^2}, \tag{3}$$

where

$\langle V \rangle$ = average voltage measured in the junction,
$I_{j\beta/2}(\gamma/2)$ = modified Bessel function of the first kind with an imaginary noninteger index,
R_N = normal resistance of the junction,
$I_c R_N = V_c$ = characteristic voltage of the junction,

and where

$$\gamma = \frac{\hbar I_c}{e k_B T}, \text{ and} \tag{4}$$

$$\beta = \frac{\hbar I_B}{e k_B T} \tag{5}$$

are dimensionless parameters involving temperature, Boltzman's constant k_B, critical current I_c, and bias current I_B. The dimensionless parameter γ is a measure of the relative intensity of thermal fluctuations given as the ratio of the Josephson coupling energy to the thermal fluctuation energy when $\beta = \gamma(I_B/I_c)$. The critical current I_c has the form[34,47]

$$I_c(T) = I_c(0)[1 - T/T_c]^{3/2} \tag{6}$$

as a function of temperature, where

T = temperature of the junction (K),

T_c = critical temperature of the junction (constant) (K), and
$I_c(0)$ = critical current at zero temperature (constant) (K),

and is valid for a long weak-link junction (see Reference 28 for power-law dependence on the junction type). A plot of Equation 3 versus temperature yields a curve with a resistive tail and a wide transition width, as shown in Figure 4.

At temperatures sufficiently close to the transition temperature, thermal fluctuations can disrupt the coupling of the phases of the wave function of two superconductors separated by a weak link. The DC Josephson current thereby acquires a noise current, resulting in a noise voltage with a nonzero average value. This nonzero average value is found using an analogy of the Brownian motion of a particle in a force field.[50,51]

A response model based on noise is useful, since earlier measurements indicate that the nonbolometric response may be due to fluctuation voltage enhancement.[5] It also allows a combination of both the weak-link region and the tightly coupled granular regions to be incorporated into a model of the granular film by assuming regions of low critical current and high critical current, respectively (see Fig. 4).

Components of the Nonbolometric Term

Figure 5 is an overview of the modeling process showing the three factors that compose the nonbolometric term (see Equation 2). Each of these three terms is described below.

Partial Derivative of Voltage with Respect to Critical Current ($\partial V/\partial I_c$)

The form of the first factor in the nonbolometric term of Equation 2, $\partial V/\partial I_c$, can be found by using Equation 3. Taking the derivative of junction voltage with respect to critical current yields

$$\frac{\partial \langle V \rangle}{\partial I_c} = -2\frac{R_N}{\pi}\frac{\sinh(\beta\pi/2)}{\left|I_{(j\beta/2)}(\gamma/2)\right|^4} \times \mathrm{Re}\left[\, I_{1+(j\beta/2)}(\gamma/2)\cdot I_{1-(j\beta/2)}(\gamma/2)\,\right], \tag{7}$$

where all parameters are defined as in Equation 3. A plot of Equation 7 versus temperature is given in Figure 5A and will be used as the first factor in the second term of Equation 2 as well as to match relative peak heights and peak positions in temperature of the measured nonbolometric response.

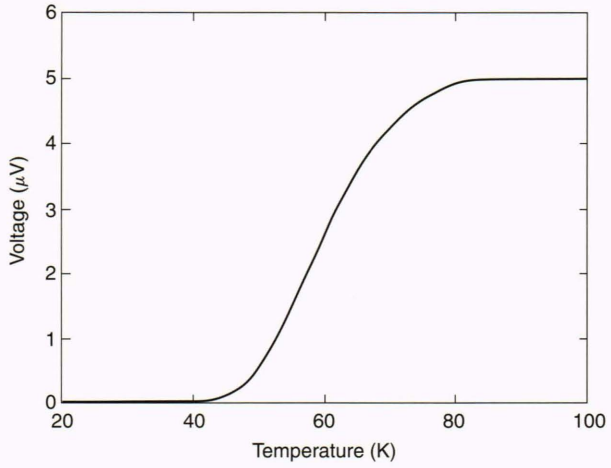

Figure 4. Thermal fluctuation voltage versus temperature. (Model parameters: superconducting energy gap = 30 meV, critical temperature = 90 K, bias current = 5 μA, critical current = 30 μA.)

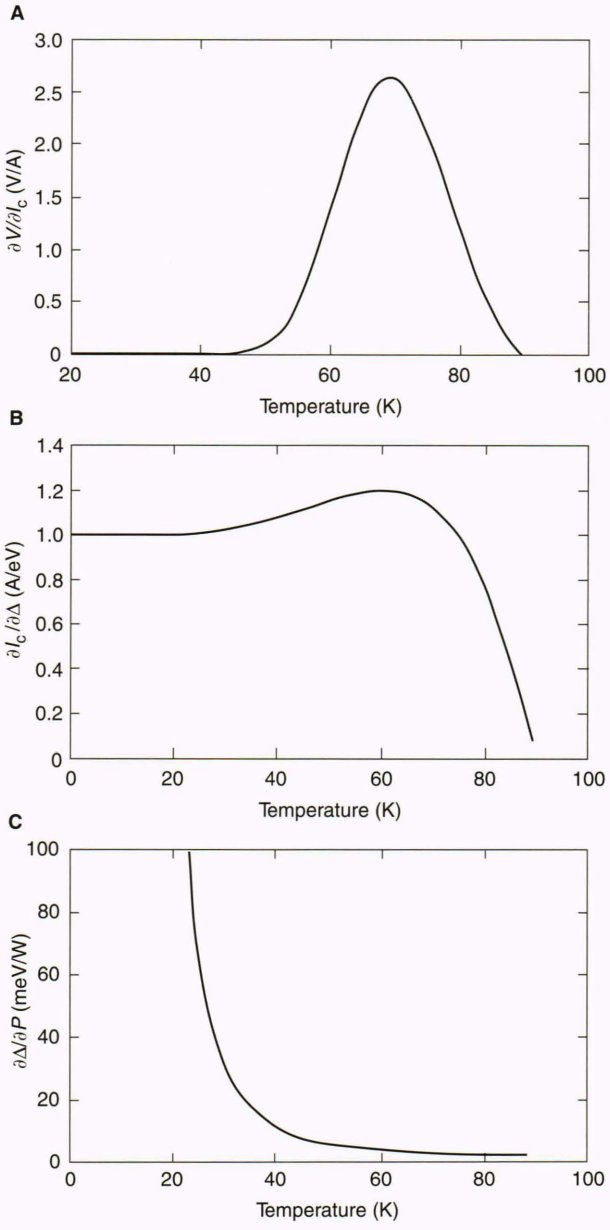

Figure 5. Overview of the modeling process showing the three components of the modeled response. Multiplying these three factors will yield the response model term versus temperature plot shown in Figure 9. **A.** Change in voltage V due to a change in junction critical current I_c. **B.** Change in critical current I_c due to a change in energy gap Δ. **C.** Change in energy gap Δ due to applied power P. (Model parameters: superconducting energy gap = 30 meV, critical temperature = 90 K, bias current = 5 μA, critical current = 30 μA.)

Partial Derivative of Critical Current with Respect to Energy Gap ($\partial I_c/\partial\Delta$)

Results from Van Duzer[34] will be used to derive the form of the second factor in the nonbolometric term of Equation 2, $\partial I_c/\partial\Delta$. A general form of I_c as a function of temperature and energy gap is given in Equation 8, although an exact form should depend on the type of junction in the sample. A critical-current equation in closed form for an SNS junction explicitly dependent on the energy gap does not exist. A Josephson tunnel junction critical-current equation was therefore used as follows:

$$I_c = \frac{G\pi}{2e}\Delta(T)f(T), \tag{8}$$

where G is the tunneling conductance and $f(T)$ is a function that depends on the type of junction. An example of a more specific form for a tunnel junction is given by Van Duzer as[34]

$$I_c = \frac{G\pi}{2e}\Delta(T)\tanh\left(\frac{\Delta(T)}{2k_BT}\right). \tag{9}$$

The behavior of this equation with respect to temperature is nearly identical to that of Equation 6 but depends explicitly on the energy gap and can be used to find the derivative of critical current with respect to energy gap as follows:

$$\frac{\partial I_c}{\partial\Delta} = \frac{G\pi}{2e}\left[\tanh\left(\frac{\Delta(T)}{2k_BT}\right) + \frac{\Delta(T)}{2k_BT}\operatorname{sech}^2\left(\frac{\Delta(T)}{2k_BT}\right)\right]. \tag{10}$$

This result is plotted versus temperature in Figure 5B and will be used as the second factor in the nonbolometric term of Equation 2.

Partial Derivative of the Energy Gap with Respect to Power ($\partial\Delta/\partial P$)

Parker[18] used results from Owen and Scalapino,[35] Rothwarf and Taylor,[52] and others[53-55] to derive the temperature-dependent form of $\partial\Delta/\partial P$, the third factor in the nonbolometric term of Equation 2, from a calculation of the quasiparticle lifetime in superconductors. We used modified results from Parker to obtain the following new expression for $\partial\Delta/\partial P$, which is valid for HTSC devices that show a fluctuation current component:

$$\frac{\partial\Delta}{\partial P} = \frac{\alpha\tau_0}{4N(0)}\left[T\exp(-2\Delta/k_BT)\right]^{-1/2}, \tag{11}$$

where α is the photoexcitation constant, τ_0 is the junction recombination parameter, and $N(0)$ is the single-spin energy density of states. This equation describes the temperature dependence of the modulation of the energy gap by incident power for a low-temperature weak-link junction and is plotted versus temperature in Figure 5C using a temperature scaling technique to account for a higher T_c. This result will be used as the third factor of the nonbolometric term of Equation 2.

MODELING RESULTS AND COMPARISON WITH MEASURED RESPONSE

In the previous section, the three factors composing the nonbolometric term were derived. The measured data can now be compared with the three factors of the nonbolometric model.

Using the fluctuation voltage model of a junction, a superconducting structure consisting of a weakened superconductor connecting two superconducting grains is used to simulate a granular film. The weakened superconductor is designed to have a relatively low critical current of 30 μA, and the two grains are modeled as strongly coupled junctions with high critical currents of 1.2 mA. The resistance of the weakened superconductor is considered small compared with a grain (the ratio of their normal junction resistances is 1:100). Figure 6 shows the resistance-versus-temperature curve employed in this model for a bias current of 1.5 μA, where the resistance was found using the fluctuation voltage and Ohm's law. The junction voltage, which depends on the bias current, is shown in Equation 3. As one can deduce from Figure 6, the resistance of the structure is dominated by the grain properties at high temperatures and by the weakened superconductor at lower temperatures, with the weakened superconductor producing the resistive tail and broad transition width.

Using this model of the granular film, one can calculate $\partial R/\partial T$ and $\partial V/\partial I_c$. In Figure 7, one can see that $\partial V/\partial I_c$ differs greatly from $\partial R/\partial T$. The $\partial R/\partial T$ in the weakened superconductor region is much smaller than the $\partial R/\partial T$ in the grain region (and is therefore not visible), indicating a bolometric response dominated by the grain and not the weakened region. This result compares well with the measured bolometric response, which did not show a large bolometric spike in the tail region. The $\partial V/\partial I_c$ is found at lower temperatures in the region of the resistive

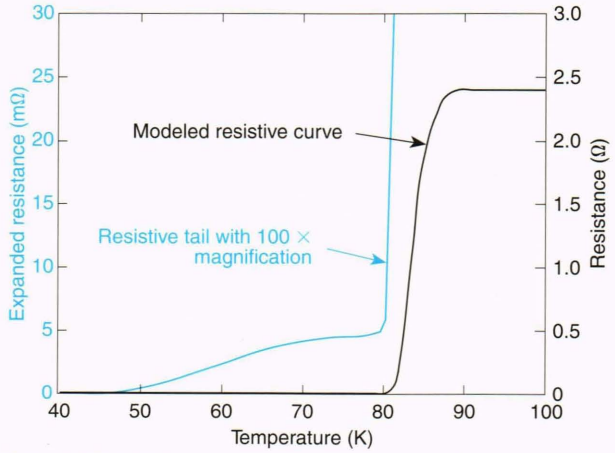

Figure 6. Resistance-versus-temperature curve for the response model showing a wide transition width and a significant resistive tail. The voltage versus temperature was found using the fluctuation voltage equation, and then the resistance versus temperature was derived using Ohm's law. (Model parameters: superconducting energy gap = 30 meV, critical temperature = 90 K, bias current = 5 μA, critical current = 30 μA.)

tail. This factor is the most critical one in the response model, since it is the only factor in the nonbolometric term largely dependent on the bias current. Its behavior dominates the nonbolometric response model, giving the peak position in temperature and approximate peak height. Figure 8 is a plot showing the behavior of the $\partial V/\partial I_c$ factor for three different bias currents. Note that the peak height increases and the peak position decreases in temperature for increasing bias current, as previously shown in measured data.[4,5]

The high-temperature component of $\partial V/\partial I_c$ (the component produced by the strongly coupled grain region) was intentionally suppressed for simplicity (on the two previous graphs, Figs. 7 and 8) by using low weighting factors. A scale factor of 8.34 was also used on each curve in this figure, since it will be needed later to match the exact peak heights of the measured data. The curves in Figures 6 through 8 are results of a single granular structure with one weakened superconducting region, as mentioned earlier. This single connection configuration limits the total allowed bias current to a value less than the critical current of a single junction. In our granular thin-film detector, the current path probably contains an array of many grains (with series and parallel connections), which allows a large bias current. For this reason, we will use an array of one hundred grain structures in parallel to allow a larger bias current and model the actual response.

When all three factors of the nonbolometric term are multiplied (to yield $\partial V/\partial P$), the results closely match the measured data, as shown in Figures 9 through 13. Figure 9 is a plot of the response model term versus temperature compared with the measured data. Here, one hundred grain structures (each with a bias current of 1.5 μA) are connected in parallel to increase the total current. One can see that a good fit results from this design. Figure 10 shows a comparison of the response model with the measured data for three bias currents. Again, a good match of peak heights and peak positions for these currents is evident.

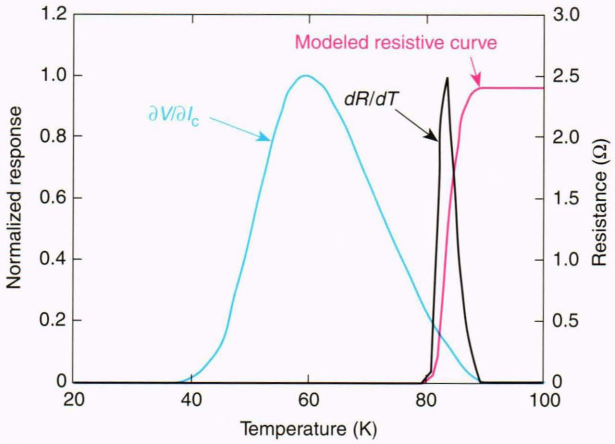

Figure 7. Comparison of $\partial V/\partial I_c$ and dR/dT showing the difference between the bolometric response model and one factor of the nonbolometric response model. (Model parameters: superconducting energy gap = 30 meV, critical temperature = 90 K, bias current = 5 μA, critical current = 30 μA, V = voltage, I_c = critical current, R = resistance, T = temperature.)

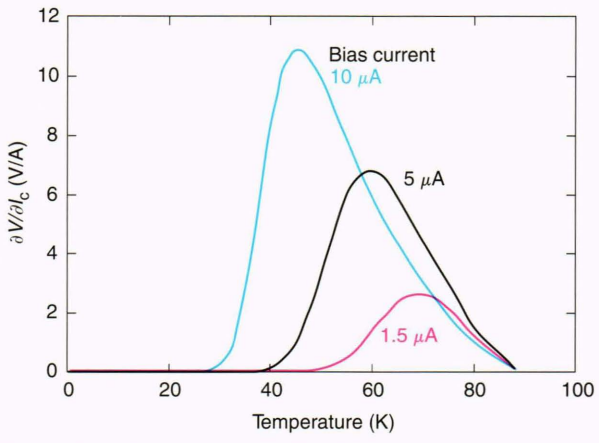

Figure 8. Behavior of the $\partial V/\partial I_c$ factor of the nonbolometric response model for three bias currents. (Model parameters: superconducting energy gap = 30 meV, critical temperature = 90 K, critical current = 30 μA, V = voltage, I_c = critical current.)

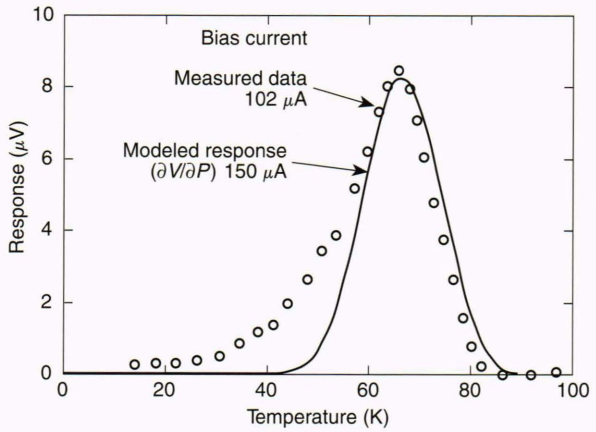

Figure 9. Comparison of measured microwave response data and modeled nonbolometric response of one hundred identical junctions in parallel. (Model parameters: superconducting energy gap = 30 meV, critical temperature = 90 K, critical current = 30 μA, bias current = 1.5 μA, V = voltage, P = power.)

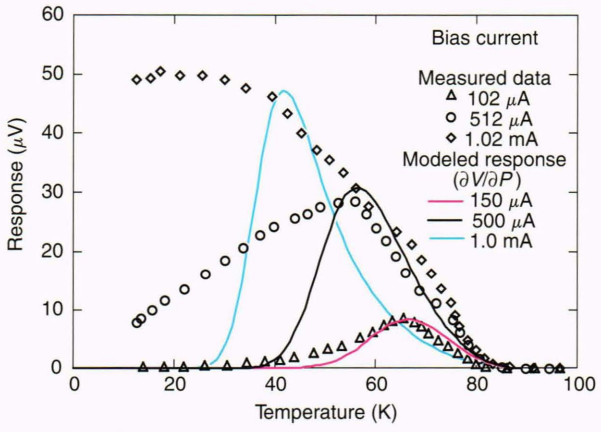

Figure 10. Comparison of measured microwave response data and modeled nonbolometric response of one hundred identical junctions in parallel for three values of bias current. (Model parameters for each identical junction: superconducting energy gap = 30 meV, critical temperature = 90 K, critical current = 30 μA, V = voltage, P = power.)

Since the $\partial\Delta/\partial P$ term is not a strong function of bias current, it does not vary significantly over the bias current range used in this model. Consequently, this term does not behave properly at high bias currents (since it is not a function of bias current, as shown in Equation 11), and a scale factor of 0.43 was needed to match the response peak height correctly at high bias current (10 μA). The peak position in temperature was correct and unmodified. The approach used to model the spreading of our measured data at high bias currents is discussed below.

The observed spreading of the microwave response at high bias currents can be explained by considering the entire film as a series of junctions with various critical currents and temperatures. As the bias current increases, a greater number of these junctions are weakened, resulting in lower critical currents and temperatures and yielding various peak heights and peak positions in temperature (i.e., a lowered critical temperature yields a response peak at a lower temperature). A sum of these various responses would then yield a spread-out response curve. This spreading effect can be calculated using a multigrain approach by modeling a number of junction structures in series (such that their voltages add in a way shown in Fig. 3) with various critical currents and critical temperatures. Calculations made using this multigrain approach indicate that careful selection of superconducting junction sections can produce a modeled response that closely matches the measured data at high current.

The modeled responses of various junction structures (having different peak heights and peaks positions, as discussed earlier) can be found that cover the entire range of the measured data, as shown in Figure 11. These curves are all Gaussian and are consistent with those shown in Figures 9 and 10. When the responses of these various structures are summed, the resulting curve (scaled by 0.5) closely matches the measured response curve, as shown in Figure 12. This calculation demonstrates that it is possible to represent a measured microwave response at high current as the response of an array of junction structures with various critical temperatures and currents. It must now be shown that the model behaves correctly for various applied powers.

Figure 13 shows the modeled response versus temperature for various incident powers. Again, one hundred grain structures (each with a bias current of 3 μA) are connected in parallel to increase the total current. A close match of peak height and peak position in temperature is seen for the low-incident-power (below saturation) response curves shown in this figure. The saturation seen in the response data at high incident powers is calculated in our model by using a height scaling factor, since the model does not inherently contain a method to calculate

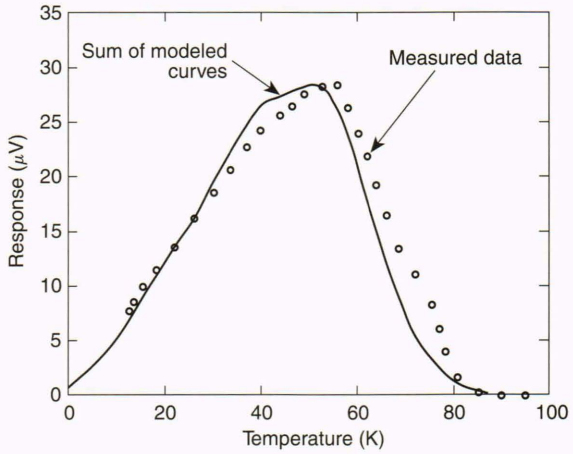

Figure 12. Comparison of measured response data and modeled multigrain response. Modeled multigrain response is the sum of the responses from the five junction structures added in series that are shown in Figure 11.

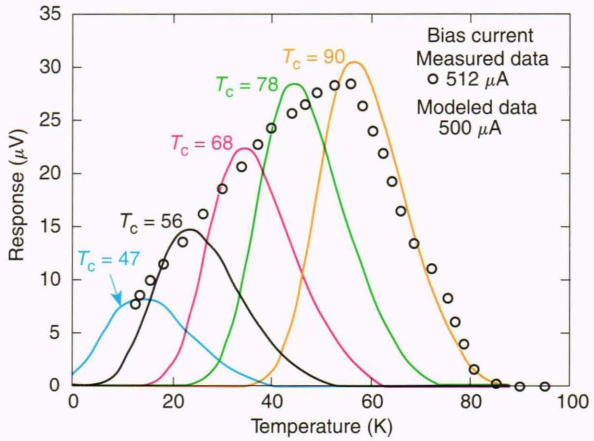

Figure 11. Comparison of measured response data and modeled response of five junction structures, each with one hundred identical junctions in parallel, placed in series so that their voltages add. The modeled response curves cover the entire range of the measured data. (Model parameters for each identical junction: superconducting energy gap = 30 meV, critical current = 30 μA, T_c = critical temperature.)

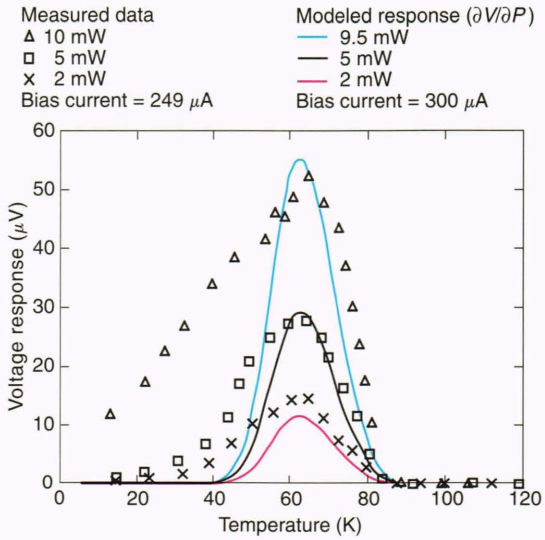

Figure 13. Comparison of measured microwave response data and modeled nonbolometric response of one hundred identical junctions in parallel for three values of incident power. (Model parameters for each identical junction: superconducting energy gap = 30 meV, critical temperature = 90 K, critical current = 30 μA; measured data parameters: microwave frequency = 9 GHz, modulation frequency = 40 Hz, V = voltage, P = power.)

the saturation values of the microwave response. Scaling factors are used for saturation to scale the modeled peak heights to match the saturated response data peak heights at high incident powers.

SUMMARY

We have described a microwave response model for a multigrain superconductor with a detection mechanism based on the thermal fluctuation voltage occurring in the networks of Josephson junctions inherent in granular films. It has been shown that data obtained through this junction model can be used to characterize our measured nonbolometric response data. These results give valuable information for the application of this nonbolometric detection mode to detectors. This model will be useful in predicting the response of a film with a controlled granular structure for which the number, size, and characteristics of the grains are known. If the growth of superconducting grains and junctions can be controlled (by laser patterning, annealing, or biepitaxial growth, for instance), it may be possible to optimize the nonbolometric response for detector applications using this response model.

REFERENCES

[1] Bednortz, J. G., and Müller, K. A., "Possible High T_c Superconductivity in the Ba-La-Cu-O System," *Z. Phys. B* **64**, 189-193(1986).

[2] Boone, B. G., *Application of High-Temperature Superconducting Thin-Film Devices to Electro-Optical and Electronic Warfare Systems,* JHU/APL TG 1377 (Feb 1990).

[3] Brasunas, J., Kunde, V., and Moseley, H., "Upcoming Planetary Missions and the Applicability of High Temperature Superconductor Bolometers," in *Proc. AMSAHTS '90–Advances in Material Science and Applications of High-Temperature Superconductors,* NASA Goddard Flight Center, Greenbelt, Md., pp. 449-458 (2-6 Apr 1990).

[4] Sova, R. M., Grabow, B. E., and Boone, B. G., "High-Temperature Superconducting Electromagnetic Radiation Detectors," *Johns Hopkins APL Tech. Dig.* **14**(1), 37-50 (1993).

[5] Grabow, B. E., *Microwave and Optical Detection Using Granular Bi-Sr-Ca-Cu-O Thin Films*, Ph.D. dissertation, The Johns Hopkins University (1992).

[6] Boone, B. G., Sova, R. M., Moorjani, K., Green, W. J., and Grabow, B. E., "Microwave Detection Using Granular Bi-Sr-Ca-Cu-O Thin Films," *J. Appl. Phys.* **69**(4), 2676-2678 (1991).

[7] Kitchin, C. R., *Astrophysical Techniques,* Adam Hilger Ltd., Bristol, pp. 17-23 (1984).

[8] Bertin, C. L., and Rose, K., "Enhanced-Mode Radiation Detection by Superconducting Films," *J. Appl. Phys.* **42**(2), 631-642 (1971).

[9] Farrel, J. N., "High-Temperature Superconducting Detector Response Model," in *Proc. Workshop on High-Temperature Superconductivity,* GACIAC PR-89-02, Huntsville, Ala., pp. 229-234 (23-25 May 1989).

[10] Ambegaokar, V., and Halperin, B. I., "Voltage Due to Thermal Noise in the DC Josephson Effect," *Phys. Rev. Lett.* **22**(25), 1364-1366 (1969).

[11] Wolf, S. A., Strom, U., and Culbertson, J. C., "Visible and Infrared Detection Using Superconductors," *Solid State Technol.,* 187-191 (Apr 1990).

[12] Strom, U., Culbertson, J. C., and Wolf, S. A., "Light Detection Using Superconducting Films," in *Proc. Workshop on High-Temperature Superconductivity,* GACIAC PR-89-02, Huntsville, Ala., pp. 219-227 (May 1989).

[13] Zaquine, I., Mage, J. C., Marcilhac, B., and Dieumegard, D., "Microwave Detection with High T_c Superconductors," *IEEE Trans. Mag.* **27**(2), 2507-2511 (Mar 1991).

[14] Richards, P. L., and Hu, Q., "Superconducting Components for Infrared and Millimeter-Wave Receivers," *Proc. IEEE* **77**(8), 1233-1246 (Aug 1989).

[15] Richards, P. L., "The Josephson Junction as a Detector of Microwave and Far Infrared Radiation," in *Semiconductors and Semimetals,* Willardson, R. K., and Beer, A. C. (eds.), Academic Press, New York, Vol. 12, pp. 395-439 (1977).

[16] Rose, K., "Superconducting FIR Detectors," *IEEE Trans. Elec. Dev.* **ED-27**, 118-125 (Jan 1980).

[17] Martin, D. H., and Bloor, D., "The Application of Superconductivity to the Detection of Radiant Energy," *Cryogenics* **1**, 159-165 (Mar 1961).

[18] Parker, W. H., "Effective Quasiparticle Lifetime in Superconducting Sn," *Solid State Comm.* **15**(6), 1003-1006 (1974).

[19] Frenkel, A., Saifi, M. A., Venkatesan, T., Lin, C., Wu, X. D., et al., "Observation of Fast Nonbolometric Optical Response of Nongranular High T_c $Y_1Ba_2Cu_3O_{7-x}$ Superconducting Thin Films," *Appl. Phys. Lett.* **54**, 1594-1596 (1989).

[20] Frenkel, A., Saifi, M. A., Venkatesan, T., England, P., Wu, X. D., et al., "Optical Response of Nongranular High-T_c $Y_1Ba_2Cu_3O_{7-x}$ Superconducting Thin Films," *J. Appl. Phys.* **67**(6), 3054-3068 (Mar 1990).

[21] Tinkham, M., "Flux Motion and Dissipation in High Temperature Superconductors," *IEEE Trans. Mag.* **27**(2), 828-832 (Mar 1991).

[22] Konopka, J., Sobolewski, R., Konopka. A., and Lewandowski, S., "Microwave Detection and Mixing in Y-Ba-Cu-O Thin Films at Liquid Nitrogen Temperatures," *Appl. Phys. Lett.* **53**, 796-798 (1988).

[23] Konopka, J., Jung, G., Gierlowski, P., Kula, W., Konopka, A., et al., "Interaction of Microwave Radiation with High-T_c Films of Different Microstructures," *Physica C* **162-164**, 1041-1042 (1989).

[24] Jung, G., Konopka, J., Gierlowski, P., and Kula, W., "Microwave Noise Emission from High T_c Thin Films," *Appl. Phys. Lett.,* **54**, 2355-2357(1989).

[25] Strom, U., Culbertson, J. C., and Wolf, S. A., "Far Infrared Photoresponse of Two-Dimensional Granular YBaCuO Films," *SPIE* **1187**, 290-294 (1989).

[26] Afanasyev, A. S., Divin, Y. Y., Gubankov, V. N., Shadrin, P. M., and Volkov, A. F., "Response of YBaCuO Thin Films to Millimeter-Wave Electromagnetic Radiation," in *Proc. Int. Conf. on Millimeter Waves and Far-IR Tech.,* McMillan, A. S., and Tucker, G. M. (eds.), Beijing, China. pp. 4-47 (Jun 1989).

[27] Afanasyev, A. S., Volkov, A. F., Gubankov, V. N., Divin, Y. Y., and Shadrin, P. M., "Response of YBaCuO Thin Films to Electromagnetic Radiation and Their Electrical Characteristics," *IEEE Trans. Mag.* **25**(2), 2571-2574 (Mar 1989).

[28] Yoshisato, Y., Takeoka, A., Ikemachi, T., Niki, K., Yokoo, T., et al., "Microwave Detector Using Granular-Type YBCO Superconductors." *Jpn. J. Appl. Phys.* **29**(6), 1080-1085 (Jun 1990).

[29] Zeldov, E., Amer, N. M., Koren, G., and Gupta, A., "Nonbolometric Optical Response of $YBa_2Cu_3O_{7-\delta}$ Epitaxial Films," *Phys. Rev. B* **39**, 9712-9714 (1989).

[30] Gallop, J. C., Radcliffe, W. J., Langham, C. D., Sobolewski, R., KuIa, W., et al., "Josephson Effects and Microwave Response of HTS Thin Films," *Physica C* **162-164**, 1545-1546 (1989).

[31] Kadin, A. M., Leung, M., Smith, A. D., and Murduck, J. M., "Infrared Photodetector Based on the Photofluxonic Effect in Superconducting Thin Films," *SPIE* **1477**, 156-165 (4 Apr 1991).

[32] Culbertson, J., Strom, U., Wolf, S. A., Skeath, P., West, E. J., et al., "Nonlinear Optical Response of Granular Y-Ba-Cu-O Films." *Phys. Rev. B.* **39**(16), 12,359-12,362 (1 Jun 1989).

[33] Strom, U., Culbertson, J. C., and Wolf, S. A., *SPIE* **1240**, 516-517 (26 Oct 1989).

[34] Van Duzer, T., and Turner, C. W., *Principles of Superconductive Devices and Circuits*, Elsevier, New York, pp. 72-92 and 139-164 (1981).

[35] Owen, C. S., and Scalapino, D. J., "Superconducting State Under the Influence of External Dynamic Pair Breaking," *Phys. Rev. Lett.* **28**(24), 1559-1560 (1972).

[36] Forrester, M. G., Talvacchio, J., and Braginski, A. I., "Electrical Response of High-T_c Superconducting Films to Laser Radiation," *Proc. GACIAC Workshop on High-T_c Superconductivity*, Huntsville, Ala. (preprint, May 1989).

[37] Kwok, H. S., Zheng, J. P., and Ying, Q. Y., "Nonthermal Optical Response of Y-Ba-Cu-O Thin Films," *Appl. Phys. Lett.* **54**(24), 2473-2475 (1989).

[38] Broklesby, W. S., Morris, D., Levi, A. F. J., Hong, M., Liou. S. H.. et al., "Electrical Response of Superconducting $YBa_2Cu_3O_{7-\delta}$ to Light," *Appl. Phys. Lett.* **54**(12), 1175-1177(1989).

[39] Leung, M., Strom, U., Culbertson, J. C., Claassen, J. H., Wolf, S. A., et al., "NbN/BN Granular Films—A Sensitive, High-Speed Detector for Pulsed Far-Infrared Radiation," *Appl. Phys. Lett.* **50**(23), 1691-1693 (Jun 1987).

[40] Ayer, W. J., and Rose, K., "Radiation Detection by Coherent Josephson Phenomena in Agglomerated Tin Films,'' *IEEE Trans. Mag.* **MAG-11**(2), 678-680 (Mar 1975).

[41] Gershenzon, E. M., Gol'tsman, G. N., Semenov, A. D., and Sergeev, A. V., "Mechanism of Picosecond Response of Granular YBaCuO Films to Electromagnetic Radiation," *IEEE Trans. Mag.* **27**(2), 1321-1324 (Mar 1991).

[42] Strom, U., Snow, E. S., Henry, R. L., Broussard, P. R., Claassen, J. H., et al., "Photoconductive Response of Granular Superconductive Films," *IEEE Trans. Mag.* **25**(2), 1315-1318 (Mar 1991).

[43] Sobolewski, R., Konopka, A., and Konopka, J., "Microwave Absorption in $YBa_2Cu_3O_{7-x}$ Thin Films," *Physica C* **153-155**, 1431-1432 (1988).

[44] Shewchun, J., and Marsh, P. F., "Performance Characteristics of Y-Ba-Cu-O Microwave Superconducting Detectors," *SPIE* **1477**, 115-138 (1991).

[45] Voss, R. F., Knoedler, C. M., and Horn, P. M., "Vortex Noise at the Superconducting Transition in Granular Aluminum Films," in *Inhomogeneous Superconductors-1979,* Gubser, D. U., Francavilla, T. L., Leibowitz, J. R., and Wolf, S. A. (eds.), American Institute of Physics, New York, pp. 314-318 (1980).

[46] Jung, G., and Konopka, J., "Josephson and Quantum Interferometer Effects in Microwave Emission from High-T_c Y-Ba-Cu-O Films," *Physica C* **162-164**, 1567-1568 (1989).

[47] Likharev, K. K., *Dynamics of Josephson Junctions and Circuits*, Gordon and Breach, Philadelphia, pp. 7-19 and 115-120 (1991).

[48] Ivanchenko, Y. M., and Zil'berman, L. A., Destruction of Josephson Current by Fluctuations," *Zh. Eksperim. i Theor. Fiz.-Pis'ma Redakt.* **8**(4), 189-192 (1968) [translated as: *JEPT Lett.* **8**, 113-115 (1968)].
[49] Ambegaokar, V., and Baratoff, A., "Tunneling Between Superconductors," *Phys. Rev. Lett.* **10**(11), 486-489 (Jun 1963), and errata, *Phys. Rev. Lett.* **11**(2), 104 (Jul 1963).
[50] Stratonovich, R. L., *Topics in the Theory of Random Noise,* Gordon and Breach, New York, pp. 62-75 (1963).
[51] Kramers, H. A., "Brownian Motion in a Field of Force and the Diffusion Model of Chemical Reactions," *Physica* **VII**(4), 284-304 (Apr 1940).
[52] Rothwarf, A., and Taylor, B. N., "Measurement of Recombination Lifetimes in Superconductors," *Phys. Rev. Lett.* **19**(1), 27-30 (1967).
[53] Parker, W. H., and Williams, W. D., "Photoexcitation of Quasiparticles in Nonequilibrium Superconductors," *Phys. Rev. Lett.* **29**(14), 924-927 (Oct 1972).
[54] Sai-Halasz, G. A., Chi, C. C., Denenstein, A., and Langenburg, D. N., "Effects of Dynamic External Pair Breaking in Superconducting Films," *Phys. Rev. Lett.* **33**, 215-218 (1974).
[55] Testardi, L. R., "Destruction of Superconductivity by Laser Light," *Phys. Rev. B* **4**(7), 2189-2196 (Oct 1971).

APPENDIX

A QUICK TUTORIAL ON SUPERCONDUCTIVITY

The two most fundamental properties of superconductors are zero DC resistance and the Meissner effect, both of which occur at temperatures below a critical temperature T_c. The Meissner effect is the ability of cooled superconductors to expel static magnetic fields and can be viewed as perfect diamagnetism up to a critical field H_c. Actually, the superconducting state of a material is associated with the values of the three parameters: temperature, current, and magnetic field. The superconducting state can be destroyed by exceeding the critical value of any one of these parameters.

In a normal metal, electrons are essentially unbound and free to move through the crystal lattice. Electron collisions with the lattice vibrations are the source of resistance and the basis of temperature-dependent losses in metals. In superconductors, when the crystal lattice is cooled to near the critical temperature T_c, electrons of opposite momentum and spin near the Fermi energy condense into bound pairs (with a lower, more favorable energy) called Cooper pairs, which exhibit zero DC resistance. The superconducting energy gap Δ is the the binding energy of the paired electrons and is also the gap that separates the sea of quasiparticles (normal electrons) from the bound pairs in the conduction band.

The superconducting state is also characterized as a collective quantum phenomenon in which the wave function

$$\psi = |\psi| \exp(j\phi) \tag{A1}$$

is a complex quantity that describes thc macroscopic superconducting state. The modulus $|\psi|$ is the superconducting order parameter, and ϕ is the phase. The modulus squared $|\psi|^2$ is n_p, the number density of Cooper pairs that constitute the supercurrent. The superconducting energy gap Δ is proportional to n_p and is typically 50 meV or less for high-temperature superconducting (HTSC) materials.

Two key length-scale parameters used to describe the superconducting slate are the coherence length and London penetration depth. The coherence length ξ_0 is a measure of the distance over which the superconducting order parameter varies, where $\xi_0 \propto 1/\Delta$. The coherence length can also be viewed as the size of a Cooper pair. For HTSC materials, it is very small (typically $\leq$ 2.7 nm). The London penetration depth λ_L is the distance a magnetic field will penetrate into the superconductor, where $\lambda_L \propto 1/n_p^{1/2}$. For HTSC materials it is approximately 200 nm.

A superconducting ring will trap flux within it when a magnetic field is present and the structure is cooled below T_c. This phenomenon is an important fundamental property for device applications. The trapped flux will induce (because of the Meissner effect) a persistent circulating (shielding) current through a depth equal to λ_L surrounding an area of normal material with a diameter at least on the order of the coherence length. The phase of the superconducting wave function changes by $2\pi n$ in going once around the ring, resulting in the quantization of the magnetic flux as measured in units of flux quanta, $\Phi_0 = h/2e$, whose magnitude is 2×10^{-15} Wb, where h is Planck's constant and e is the electron charge. These flux quanta manifest themselves as vortices or fluxons, especially in certain types of thin films.

Another fundamental effect observed in superconductors of practical importance for devices is the Josephson effect, which is noted when two pieces of superconductor are separated by a thin region of weak metallic superconductor (where the order parameter is reduced) or by an insulator through which Cooper pairs can tunnel. The Josephson critical current I_c is the largest flow of Cooper pairs allowed through the junction without losses. When a current less than I_c flows through the junction, Cooper pairs tunnel through the barrier, establishing a phase change ($\Delta\phi$) between the wave functions on each side of the junction, which results in a current given by

$$I = I_c \sin \Delta\phi \ . \tag{A2}$$

When I exceeds I_c, the phase difference evolves in time according to

$$d\,\Delta\phi/dt = 4\pi eV/h \ , \tag{A3}$$

where V is the voltage across the junction and h is Planck's constant, and then current no longer flows without losses. In this case an AC component of current is added to I_c at a frequency proportional to the voltage across the junction. Josephson junctions exhibit inherent nonlinear properties that can be used in the detection of radiant energy.

THE AUTHORS

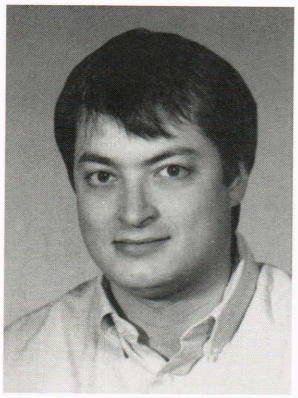

BARRY E. GRABOW received his B.S. in electrical engineering from the Milwaukee School of Engineering in 1987 and an M.S. and Ph.D. in electrical engineering from The Johns Hopkins University in 1990 and 1992, respectively. In 1992, he held a postdoctoral position in the Electrical and Computer Engineering Department of The Johns Hopkins University for one semester. Dr. Grabow's current interests include superconductivity, microwaves, optics, and solid-state physics. He is presently teaching at The Johns Hopkins University for the Part-time Programs in Engineering and Applied Sciences and works in the Electro-Optical Systems Group at APL. Dr. Grabow holds memberships in Tau Beta Pi, Eta Kappa Nu, Delta Sigma Phi, and SPIE.

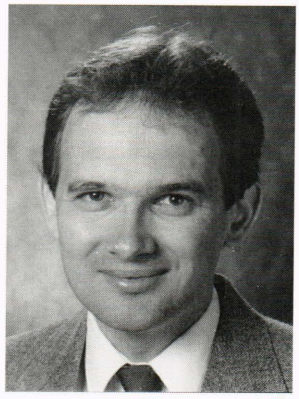

BRADLEY G. BOONE is supervisor of the Image and Signal Processing Section of APL's Electro-Optical Systems Group. He received his Ph.D. in physics from the University of Virginia in 1977, working in superconducting electronics with Bascom S. Deaver. Since joining APL in 1977, he has worked on a variety of projects related to lasers, optical and infrared sensors, imaging radar, optical pattern recognition, and high-temperature superconductivity. Dr. Boone is on the faculty of The Johns Hopkins University G.W.C. Whiting School of Engineering and was a William S. Parsons visiting professor in the Electrical and Computer Engineering Department of JHU in 1991. He holds membership in SPIE.

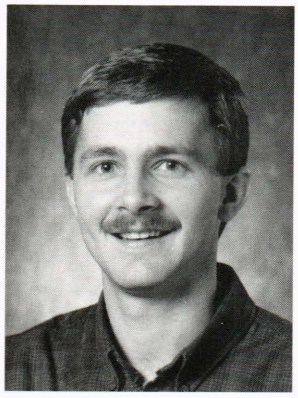

RAYMOND M. SOVA received his B.S. in electrical engineering from the Pennsylvania State University and his M.S. in applied physics from The Johns Hopkins University. He is currently pursuing a Ph.D. in electrical engineering from The Johns Hopkins University. He is a member of APL's Electro-Optical Systems Group, where he has worked on the development of a digital signal processing algorithm for electronically scaling and rotating digital images and the development of high-temperature (>77 K) superconducting thin-film radiation detectors. Current research interests include the development of a laser remote sensing system for measuring atmospheric humidity and temperature profiles and spectroscopic studies of oxide materials and atmospheric gases.